Enhanced Low-Complexity FDD System Feedback with Variable Bit Lengths via Generative Modeling

Nurettin Turan, Benedikt Fesl, and Wolfgang Utschick

TUM School of Computation, Information and Technology, Technical University of Munich, Germany

Email: {nurettin.turan, benedikt.fesl, utschick}@tum.de

Abstract—Recently, a versatile limited feedback scheme based on a Gaussian mixture model (GMM) was proposed for frequency division duplex (FDD) systems. This scheme provides high flexibility regarding various system parameters and is applicable to both point-to-point multiple-input multiple-output (MIMO) and multi-user MIMO (MU-MIMO) communications. The GMM is learned to cover the operation of all mobile terminals (MTs) located inside the base station (BS) cell, and each MT only needs to evaluate its strongest mixture component as feedback, eliminating the need for channel estimation at the MT. In this work, we extend the GMM-based feedback scheme to variable feedback lengths by leveraging a single learned GMM through merging or pruning of dispensable mixture components. Additionally, the GMM covariances are restricted to Toeplitz or circulant structure through model-based insights. These extensions significantly reduce the offloading amount and enhance the clustering ability of the GMM which, in turn, leads to an improved system performance. Simulation results for both point-to-point and multi-user systems demonstrate the effectiveness of the proposed extensions.

Index Terms—Gaussian mixture models, machine learning, limited feedback, precoding, frequency division duplexing.

I. INTRODUCTION

In the next generation of cellular systems (6G), the BS has the ability to adjust to changing channel conditions. However, in FDD systems, this adaptation must rely on feedback from the MT since channel reciprocity is not maintained [1]. There is considerable interest in systems that use limited feedback, where only a few bits are designated [1]. In this context, two main strategies can be distinguished. The first involves estimating the downlink (DL) channel at the MTs and determining the feedback based on this [1]–[3]. The second approach aims to directly encode feedback from pilot observations, such as through deep learning, cf., e.g., [4], [5].

In recent works, a versatile GMM-based limited feedback scheme was proposed which provides flexibility with respect to the number of antennas, the transmission mode, the number of MTs, the supported signal-to-noise ratio (SNR) range, the number of pilots, and the choice of the precoding algorithm, together with low complexity to determine the feedback by circumventing the necessity for channel estimation at the MTs [6], [7]. The MTs, select the index of the GMM component

with the highest responsibility (posterior probability) for their received pilot signal as their feedback information. The corresponding GMM is learned from data which represent the underlying channel distribution of a whole communication scenario inside a BS cell. This is motivated by the universal approximation property [8] and the strong results of GMMs in wireless communications [9]–[12]. A main advantage is that the offline fitting of the GMM can be done centralized at the BS due to the absence of a distributional shift between the channel distributions of uplink (UL) and DL, cf. [13]–[15].

Although GMMs possess the universal approximation property, cf. [8], a known trait is that their corresponding mixture components may not be distinct enough from each other to be interpreted as clusters [16]. This similarly also arises in the GMM-based feedback scheme from [7], where the number K of mixture components is predetermined by the number B of feedback bits, i.e., $K = 2^B$. Therefore, the GMM should exhibit both a strong clustering ability for selecting the feedback index and a good likelihood model for the underlying channel distribution of the communication scenario, while maintaining a fixed number of components. To address this problem, various merging and pruning techniques have been proposed in the literature [16], [17]. Furthermore, structural features of the covariance matrices, imposed by the antenna arrays, can be utilized in order to reduce the number of parameters of the GMM which, in turn, leads to a higher robustness against overfitting for a limited amount of training data [11].

Contributions: This work extends the versatile GMM-based feedback scheme from [6], [7] by leveraging a single learned GMM to variable feedback bit lengths through merging or pruning of dispensable mixture components. Thereby, a simple pruning technique and a merging approach—which combines components with high similarity—is analyzed. Additionally, we investigate the restriction of the GMM to Toeplitz- and circulant-structured covariances which drastically reduces the necessary offloading overhead from the BS to the MTs and prevents overfitting in the case of limited training data. Simulation results show that the reduction of GMM components through merging or pruning enables variable bit lengths and is superior to directly fitting a smaller GMM because of the enhanced clustering ability. Furthermore, the structured GMM variants yield great performances with low memory overhead for both point-to-point and MU-MIMO systems.

II. System and Channel Models

A. Data Transmission Phase – Point-to-Point MIMO System

In a point-to-point MIMO system the DL received signal is $\boldsymbol{y}' = \boldsymbol{H}\boldsymbol{x} + \boldsymbol{n}'$, where $\boldsymbol{y}' \in \mathbb{C}^{N_\mathrm{rx}}$ is the receive vector, $\boldsymbol{x} = \boldsymbol{Q}^{1/2}\boldsymbol{s} \in \mathbb{C}^{N_\mathrm{tx}}$ with $\mathrm{E}[\boldsymbol{s}\boldsymbol{s}^\mathrm{H}] = \boldsymbol{I}_{N_\mathrm{tx}}$ is the precoded transmit vector, $\boldsymbol{H} \in \mathbb{C}^{N_\mathrm{rx} \times N_\mathrm{tx}}$ is the MIMO channel with $N_\mathrm{rx} < N_\mathrm{tx}$, and $\boldsymbol{n}' \sim \mathcal{N}_\mathbb{C}(\boldsymbol{0}, \sigma_n^2 \boldsymbol{I}_{N_\mathrm{rx}})$ denotes the additive white Gaussian noise (AWGN). In a limited feedback system, B bits are used for encoding the feedback index $k^\star \in \{1, 2, \cdots, 2^B\}$ that specifies an element from a codebook of 2^B pre-computed transmit covariance matrices $\mathcal{Q} = \{\boldsymbol{Q}_1, \boldsymbol{Q}_2, \ldots, \boldsymbol{Q}_{2^B}\}$ [1].

B. Data Transmission Phase – Multi-user MIMO System

We utilize linear precoding in a single-cell MU-MIMO DL system. The BS is equipped with N_tx transmit antennas and each MT $j \in \mathcal{J} = \{1, 2, \ldots, J\}$, is equipped with N_rx antennas. The precoded DL data vector is $\boldsymbol{x} = \sum_{j=1}^{J} \boldsymbol{M}_j \boldsymbol{s}_j$, where $\boldsymbol{s}_j \in \mathbb{C}^{d_j}$ is the transmit signal of MT j, with $\mathrm{E}[\boldsymbol{s}_j] = \boldsymbol{0}$ and $\mathrm{E}[\boldsymbol{s}_j \boldsymbol{s}_j^\mathrm{H}] = \boldsymbol{I}_{d_j}$, and $\boldsymbol{M}_j \in \mathbb{C}^{N_\mathrm{tx} \times d_j}$ is the precoding matrix of MT j. The precoders fulfill $\mathrm{tr}(\sum_{j=1}^{J} \boldsymbol{M}_j \boldsymbol{M}_j^\mathrm{H}) = \rho$. In the multi-user setup, each MT reports its own feedback information $k_j^\star$ to the BS, which then jointly designs the precoders $\boldsymbol{M}_j$.

C. Pilot Transmission Phase

During the pilot transmission phase, every MT indexed as $j \in \mathcal{J}$ receives

$$\boldsymbol{Y}_j = \boldsymbol{H}_j \boldsymbol{P} + \boldsymbol{N}_j \in \mathbb{C}^{N_\mathrm{rx} \times n_p} \tag{1}$$

where $\boldsymbol{N}_j = [\boldsymbol{n}'_{j,1}, \ldots, \boldsymbol{n}'_{j,n_p}] \in \mathbb{C}^{N_\mathrm{rx} \times n_p}$ with $\boldsymbol{n}'_{j,p} \sim \mathcal{N}_\mathbb{C}(\boldsymbol{0}, \sigma_j^2 \boldsymbol{I}_{N_\mathrm{rx}})$, for $p \in \{1, 2, \ldots, n_p\}$ and n_p is the number of pilots, where we consider $n_p \leq N_\mathrm{tx}$. It is assumed that the BS employs a uniform rectangular array (URA). Hence, we utilize a 2D-DFT sub-matrix as the pilot matrix, cf., e.g., [7]. To maintain the power constraint each column $\boldsymbol{p}_p$ of $\boldsymbol{P}$ is normalized: $\|\boldsymbol{p}_p\|^2 = \rho$. For the subsequent analysis, it is advantageous to vectorize (1): $\boldsymbol{y}_j = \boldsymbol{A}\boldsymbol{h}_j + \boldsymbol{n}_j$, where $\boldsymbol{h}_j = \mathrm{vec}(\boldsymbol{H}_j)$, $\boldsymbol{y}_j = \mathrm{vec}(\boldsymbol{Y}_j)$, $\boldsymbol{n}_j = \mathrm{vec}(\boldsymbol{N}_j)$, $\boldsymbol{A} = \boldsymbol{P}^\mathrm{T} \otimes \boldsymbol{I}_{N_\mathrm{rx}}$ and $\boldsymbol{n}_j \sim \mathcal{N}_\mathbb{C}(\boldsymbol{0}, \boldsymbol{\Sigma})$ with $\boldsymbol{\Sigma} = \sigma_n^2 \boldsymbol{I}_{N_\mathrm{rx} n_p}$. In case of a point-to-point MIMO system, we simplify notation for convenience by omitting the index j, resulting in

$$\boldsymbol{y} = \boldsymbol{A}\boldsymbol{h} + \boldsymbol{n} \in \mathbb{C}^{N_\mathrm{rx} n_p}. \tag{2}$$

To simplify notation further, we will use the channel matrix $\boldsymbol{H}$ and its vectorized form $\boldsymbol{h}$ interchangeably.

D. Channel Model and Data Generation

The QuaDRiGa channel simulator [18] is used to create a training dataset

$$\mathcal{H} = \{\boldsymbol{h}_\ell = \mathrm{vec}(\boldsymbol{H}_\ell)\}_{\ell=1}^{L} \tag{3}$$

consisting of L channel realizations for the above system model. Since we utilize the same simulation setup, we refer the reader to [7] for more details.

III. GMM-based Limited Feedback Scheme

A. GMM Preliminaries

A GMM is a probability density function (PDF) of the form

$$f_{\boldsymbol{h}}^{(K)}(\boldsymbol{h}) = \sum_{k=1}^{K} \pi_k \mathcal{N}_\mathbb{C}(\boldsymbol{h}; \boldsymbol{\mu}_k, \boldsymbol{C}_k) \tag{4}$$

where each term within the summation represents one of its K constituent *components*. The maximum likelihood estimates for the GMM's parameters, which include the mixing coefficients π_k, means $\boldsymbol{\mu}_k$, and covariances $\boldsymbol{C}_k$, can be calculated by utilizing a training dataset $\mathcal{H}$ as described in (3), along with an expectation maximization (EM) algorithm outlined in [19, Subsec. 9.2.2]. GMMs enable the computation of *responsibilities* [19, Sec. 9.2],

$$p(k \mid \boldsymbol{h}) = \frac{\pi_k \mathcal{N}_\mathbb{C}(\boldsymbol{h}; \boldsymbol{\mu}_k, \boldsymbol{C}_k)}{\sum_{i=1}^{K} \pi_i \mathcal{N}_\mathbb{C}(\boldsymbol{h}; \boldsymbol{\mu}_i, \boldsymbol{C}_i)} \tag{5}$$

which represent the posterior probability that a particular $\boldsymbol{h}$ originates from component k. The inherent joint Gaussianity of each GMM component and the AWGN enables the simple computation of the GMM of the observations by utilizing the GMM from (4) as

$$f_{\boldsymbol{y}}^{(K)}(\boldsymbol{y}) = \sum_{k=1}^{K} \pi_k \mathcal{N}_\mathbb{C}(\boldsymbol{y}; \boldsymbol{A}\boldsymbol{\mu}_k, \boldsymbol{A}\boldsymbol{C}_k \boldsymbol{A}^\mathrm{H} + \boldsymbol{\Sigma}). \tag{6}$$

Analogously, we can compute:

$$p(k \mid \boldsymbol{y}) = \frac{\pi_k \mathcal{N}_\mathbb{C}(\boldsymbol{y}; \boldsymbol{A}\boldsymbol{\mu}_k, \boldsymbol{A}\boldsymbol{C}_k \boldsymbol{A}^\mathrm{H} + \boldsymbol{\Sigma})}{\sum_{i=1}^{K} \pi_i \mathcal{N}_\mathbb{C}(\boldsymbol{y}; \boldsymbol{A}\boldsymbol{\mu}_i, \boldsymbol{A}\boldsymbol{C}_i \boldsymbol{A}^\mathrm{H} + \boldsymbol{\Sigma})}. \tag{7}$$

B. Point-to-Point MIMO System

In an offline phase, firstly, a codebook $\mathcal{Q} = \{\boldsymbol{Q}_k\}_{k=1}^{K}$, with $K = 2^B$, is constructed based on the GMM $f_{\boldsymbol{h}}^{(K)}$ from (4) that is learned from the dataset (3). Therefore, by utilizing the GMM, the training data are clustered according to their GMM responsibilities. That is, $\mathcal{H}$ is partitioned into K disjoint sets

$$\mathcal{V}_k = \{\boldsymbol{h} \in \mathcal{H} \mid p(k \mid \boldsymbol{h}) \geq p(j \mid \boldsymbol{h}) \text{ for } k \neq j\} \tag{8}$$

for $k = 1, \ldots, K$. Then each codebook entry is determined:

$$\boldsymbol{Q}_k = \arg\max_{\boldsymbol{Q} \succeq \boldsymbol{0}} \frac{1}{|\mathcal{V}_k|} \sum_{\mathrm{vec}(\boldsymbol{H}) \in \mathcal{V}_k} r(\boldsymbol{H}, \boldsymbol{Q}) \tag{9}$$

$$\text{subject to} \quad \mathrm{tr}(\boldsymbol{Q}) \leq \rho$$

where the spectral efficiency is

$$r(\boldsymbol{H}, \boldsymbol{Q}) = \log_2 \det\left(\boldsymbol{I} + \frac{1}{\sigma_n^2} \boldsymbol{H}\boldsymbol{Q}\boldsymbol{H}^\mathrm{H}\right). \tag{10}$$

A projected gradient ascent algorithm is utilized to solve this optimization problem, cf. [7]. In the online phase, explicit channel estimation is circumvented and the pilot observation $\boldsymbol{y}$ is used to determine the feedback index via:

$$k^\star = \arg\max_{k} p(k \mid \boldsymbol{y}). \tag{11}$$

The computational complexity for determining the feedback via (11) by using the GMM is $\mathcal{O}(K N_\mathrm{rx}^2 n_p^2)$, cf. [7]. Thus, the complexity is not affected by N_tx, which is particularly beneficial for massive MIMO systems. It's worth noting that

parallelization is possible, given that the evaluation of all K responsibilities can be conducted independently. The MT solely needs the GMM parameters for calculating (11) and does not require any codebook knowledge. Furthermore, the GMM of the observations in (6) can be easily customized at the MT to accommodate various SNR levels and pilot configurations, by simply updating the means and covariances, cf. (6), without the need for retraining. As a baseline for performance analysis, perfect channel state information (CSI) can be used to determine the feedback

$$k^\star = \arg\max_k \ p(k \mid \boldsymbol{h}). \tag{12}$$

C. Multi-User MIMO System

In [7] it was shown that directional information associated with each codebook entry can be obtained by conducting a singular value decomposition (SVD), i.e., $\boldsymbol{Q}_k = \boldsymbol{X}_k \boldsymbol{T}_k \boldsymbol{X}_k^{\mathrm{H}}$. Thereby, the matrix $\boldsymbol{T}_k$ arranges the singular values in descending order, while the matrix $\bar{\boldsymbol{X}}_k$ encompasses the first N_{rx} vectors of $\boldsymbol{X}_k$ as the relevant directional information. Consequently, the set $\mathcal{Q} = \{\bar{\boldsymbol{X}}_1, \bar{\boldsymbol{X}}_2, \cdots, \bar{\boldsymbol{X}}_K\}$ forms a directional codebook, cf. [7]. Utilizing the GMM-based approach each MT efficiently computes its feedback by:

$$k_j^\star = \arg\max_k \ p(k \mid \boldsymbol{y}_j). \tag{13}$$

Every MT transmits the index $k_j^\star$ to the BS, which subsequently represents each MT's channel with the subspace information linked with the corresponding codebook entry $\widetilde{\boldsymbol{H}}_j = \bar{\boldsymbol{X}}_{k_j^\star}^{\mathrm{H}}$. The BS can then utilize widely-used precoding techniques, such as the iterative weighted minimum mean square error (WMMSE) [20], in order to jointly design the precoders, cf. [7].

Alternatively, an approach based on generative modeling was also introduced in [7]. In this approach, the channel matrix of each MT is treated as a random variable, and the precoders are computed using the stochastic WMMSE (SWMMSE) algorithm [21]. The GMM-based approach is able to generate samples that adhere to the channel's distribution due to the inherent sample generation capability of GMMs. Specifically, given the feedback $k_j^\star$ of each MT, see (13), one can generate samples through $\boldsymbol{h}_{j,\mathrm{sample}} \sim \mathcal{N}_{\mathbb{C}}(\boldsymbol{\mu}_{k_j^\star}, \boldsymbol{C}_{k_j^\star})$, which conveys statistical information about the channel of MT j. By applying the SWMMSE algorithm, the BS can compute the precoders by utilizing the generated samples, cf. [7].

IV. ENABLING VARIABLE BIT LENGTHS

In this Section, we discuss how the GMM-based feedback scheme can be enabled to utilize variable bit lengths by only requiring a single GMM of a certain size, of which GMMs with a smaller number of components can be obtained. We investigate two different mixture reduction techniques, where given a GMM with $K = 2^B$ components, another GMM with fewer components $K_S = 2^{B_S}$, with, $K_S < K$, can be obtained.

Algorithm 1 Variable Bit Lengths Enabled Through Merging.

Require: GMM with $K = 2^B$ components. Desired number of components $K_S = 2^{B_S}$ with $K_S < K$.
1: $i = K$ {track number of GMM components}
2: **repeat**
3:    Calc. moment preserving merge of all pairs of components using (14).
4:    Find pair with smallest dissimilarity $d_{a,b}$, via (15).
5:    Replace this pair by their moment preserving merge.
6:    $i \leftarrow i - 1$
7: **until** $i = K_S$
8: Partition $\mathcal{H}$ into K_S disjoint sets $\mathcal{V}_k$ with $k = 1, \dots, K_S$ according to the GMM responsibilities, cf. (8).
9: Compute codebook $\mathcal{Q} = \{\boldsymbol{Q}_k\}_{k=1}^{K_S}$ by solving (9) for each entry.

Algorithm 2 Variable Bit Lengths Enabled Through Pruning.

Require: GMM with $K = 2^B$ components. Desired number of components $K_S = 2^{B_S}$ with $K_S < K$.
1: Remove the $K - K_S$ components with smallest mixing coefficients π_k.
2: Re-normalize remaining mixing coefficients to one.
3: Discard codebook entries correspondingly and obtain $\mathcal{Q} = \{\boldsymbol{Q}_k\}_{k=1}^{K_S}$.

There exist many methods to obtain a GMM with fewer components starting from a GMM with more components. In this work, we analyze two types of mixture reduction techniques. In particular, we use one *merging* strategy which successively combines pairs of components with high similarity [17] and one *pruning* strategy, which simply discards components with a low contribution to the overall mixture [22].

In this work, we focus our analysis on the merging technique from [17]. Thereby, one replaces two mixture components with the smallest dissimilarity denoted by $\{\pi_a, \boldsymbol{\mu}_a, \boldsymbol{C}_a\}$ and $\{\pi_b, \boldsymbol{\mu}_b, \boldsymbol{C}_b\}$, by their moment preserving merge $\{\pi_m, \boldsymbol{\mu}_m, \boldsymbol{C}_m\}$ [17]:

$$\begin{aligned} \pi_m &= \pi_a + \pi_b \\ \boldsymbol{\mu}_m &= \tfrac{1}{\pi_m}(\pi_a \boldsymbol{\mu}_a + \pi_b \boldsymbol{\mu}_b) \\ \boldsymbol{C}_m &= (\tfrac{\pi_a}{\pi_m} \boldsymbol{C}_a + \tfrac{\pi_b}{\pi_m} \boldsymbol{C}_b + \tfrac{\pi_a \pi_b}{\pi_m^2}(\boldsymbol{\mu}_a - \boldsymbol{\mu}_b)(\boldsymbol{\mu}_a - \boldsymbol{\mu}_b)^{\mathrm{H}}) \end{aligned} \tag{14}$$

The dissimilarity between two components is measured by

$$\begin{aligned} d_{a,b} = \tfrac{1}{2}[\pi_m \log\det(\boldsymbol{C}_m) \\ - \pi_a \log\det(\boldsymbol{C}_a) - \pi_b \log\det(\boldsymbol{C}_b)] \end{aligned} \tag{15}$$

which is an upper bound on the Kullback-Leibler divergence between the GMMs before and after the merge, cf. [17]. The merging procedure is successively repeated until a GMM of the desired size is obtained, i.e., when the number of GMM components is reduced to 2^{B_S}. After a GMM of the desired size is obtained, the corresponding codebook needs to be constructed at the BS in the same way as described in Section III-B. Algorithm 1 summarizes the merging procedure and the accompanying codebook construction.

The pruning strategy simply removes $K - K_S$ components with the smallest mixing coefficient π_k (see (4)), and the mixing coefficients of the remaining components are re-normalized to one [22]. A main advantage of the pruning strategy is its low computational complexity. In particular, it only requires traversing a list of sorted mixing coefficients. In this case, an updated codebook $\mathcal{Q} = \{\boldsymbol{Q}_k\}_{k=1}^{K_S}$ can simply be

Name	Covariance Parameters	Example
Full	$\frac{1}{2}KN(N+1)$	$8.4 \cdot 10^6$
Kronecker	$\frac{1}{2}K_{\mathrm{rx}}N_{\mathrm{rx}}(N_{\mathrm{rx}}+1) + \frac{1}{2}K_{\mathrm{tx}}N_{\mathrm{tx}}(N_{\mathrm{tx}}+1)$	$9.0 \cdot 10^3$
Toeplitz	$2K_{\mathrm{rx}}N_{\mathrm{rx}} + 4K_{\mathrm{tx}}N_{\mathrm{tx}}$	$2.1 \cdot 10^3$
Circulant	$K_{\mathrm{rx}}N_{\mathrm{rx}} + K_{\mathrm{tx}}N_{\mathrm{tx}}$	$5.7 \cdot 10^2$

TABLE I: Analysis of the number of covariance parameters of the (structured) GMM.

Fig. 1: Flowchart of the improved versatile feedback scheme. Red (blue) colored nodes are processed at the BS (MTs) and solid (dashed) arrows indicate online (offline) processing.

obtained by discarding the respective codebook entries which correspond to the removed GMM components. Algorithm 2 summarizes the pruning procedure.

V. REDUCING THE OFFLOADING OVERHEAD

To enable a MT to compute feedback indices via (11), the parameters of the GMM need to be offloaded to the MT upon entering the BS' coverage area, cf. [7]. To reduce the offloading overhead model-based insights can be utilized to obtain structured covariances with fewer parameters. For example, one can constrain the GMM covariances to a Kronecker factorization of the form $C_k = C_{\mathrm{tx},k} \otimes C_{\mathrm{rx},k}$ which has no notable impact on the performance, cf. [7], [9]. In this context, instead of fitting an unconstrained GMM with $N \times N$-dimensional covariances, a GMM specific to the transmit side and another for the receive side is fitted. These transmit-side and receive-side GMMs have $N_{\mathrm{tx}} \times N_{\mathrm{tx}}$ and $N_{\mathrm{rx}} \times N_{\mathrm{rx}}$-dimensional covariances respectively, with K_{tx} and K_{rx} components. Subsequently, by computing all Kronecker products of the corresponding transmit-side and receive-side covariance matrices, a $K = K_{\mathrm{tx}}K_{\mathrm{rx}}$-components GMM with $N \times N$-dimensional covariances is obtained.

In this work, we investigate the incorporation of further structural features to the transmit- and receive-side GMM covariance matrices imposed by the antenna structure at the transmitter or the receiver. In case of a uniform linear array (ULA), it is common to assume a Toeplitz covariance matrix, which for a large number of antenna elements, is well approximated by a circulant matrix, cf., e.g., [12]. If a URA is deployed, the structural assumptions result in block-Toeplitz matrices with Toeplitz blocks, or block-circulant matrices with circulant blocks, respectively [12].

In the assumed case of a URA employed at the BS with $N_{\mathrm{tx,v}}$ vertical and $N_{\mathrm{tx,h}}$ horizontal ($N_{\mathrm{tx}} = N_{\mathrm{tx,v}}N_{\mathrm{tx,h}}$) elements, the structured covariances can be expressed as $C_{\mathrm{tx},k} = D^{\mathrm{H}} \operatorname{diag}(c_{\mathrm{tx},k})D$, where on the one hand, when assuming a Toeplitz structure, $D = D_{N_{\mathrm{tx,v}}} \otimes D_{N_{\mathrm{tx,h}}}$, where D_T contains the first T columns of a $2T \times 2T$ discrete Fourier transform (DFT) matrix, and $c_{\mathrm{tx},k} \in \mathbb{R}_+^{4N_{\mathrm{tx}}}$ [11], [12]. On the other hand, when assuming circular structure, we have $D = F_{N_{\mathrm{tx,v}}} \otimes F_{N_{\mathrm{tx,h}}}$, where F_T is the $T \times T$ DFT-matrix, and $c_{\mathrm{tx},k} \in \mathbb{R}_+^{N_{\mathrm{tx}}}$. At the MTs, we assume to have ULAs, thus D contains either the first N_{rx} columns of a $2N_{\mathrm{rx}} \times 2N_{\mathrm{rx}}$ DFT matrix and correspondingly $c_{\mathrm{rx},k} \in \mathbb{R}_+^{2N_{\mathrm{rx}}}$ (Toeplitz), or $D = F_{N_{\mathrm{rx}}}$ and $c_{\mathrm{rx},k} \in \mathbb{R}_+^{N_{\mathrm{rx}}}$ (circulant). With these structural constraints the GMM covariances are fully determined by the vectors $c_{\{\mathrm{tx,rx}\},k}$. Overall, these insights significantly reduce
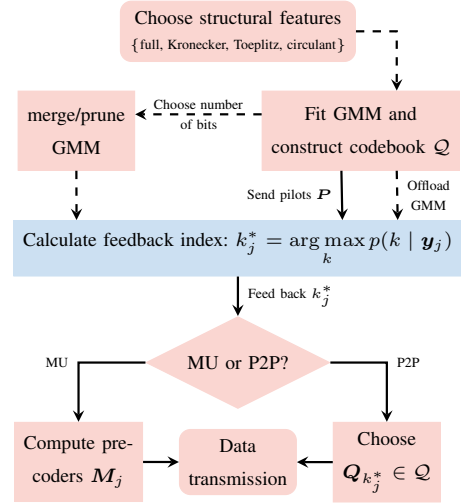
the offloading overhead, enable a reduced complexity in offline training, facilitate parallelization of the fitting process, and require fewer training samples since fewer parameters need to be learned, cf. [11], [12].

Table I depicts the number of (structured) GMM covariance parameters (accounting for symmetries). We use exemplarily the simulation parameters of a configuration with $B = 6$, $(N_{\mathrm{tx}}, N_{\mathrm{rx}}) = (32, 16)$, and $(K_{\mathrm{tx}}, K_{\mathrm{rx}}) = (16, 4)$, which we consider in Section VII. We can observe that, structural constraints significantly reduce the offloading overhead.

VI. DISCUSSION ON THE ENHANCED VERSATILITY

The low-complexity GMM-based feedback scheme from [7] exhibits great flexibility with respect to the transmission mode, i.e., either point-to-point MIMO or MU-MIMO, the supported range of SNR values, the pilot configuration, and the selection of the precoding algorithm, but utilizes a GMM with a predefined number of components $K = 2^B$. In principle, the BS could offload many GMMs with different sizes, which would allow for different numbers of feedback bits. However, the corresponding signaling overhead might be unaffordable in practice. Therefore, in Section IV we discussed different mixture reduction techniques and their corresponding codebook update procedures. Particularly, given a GMM with $K = 2^B$ components, GMMs with fewer components $K_S = 2^{B_S}$, i.e, $K_S < K$, can be obtained. Accordingly, the scheme is enabled to support variable bit lengths by successively decreasing the number of components and thereby the number of feedback bits starting from B bits ($B - 1, B - 2, \cdots$). Due to the simplicity of the pruning strategy, it can be straightforwardly implemented at the MTs. The merging strategy can be either conducted at the MTs, or to reduce their computational burden, the BS could offload additional lists with the respective merging updates. Moreover, the MT only requires the GMM and does not need to be aware of the codebook in order to compute the feedback via (11). Altogether, this allows for
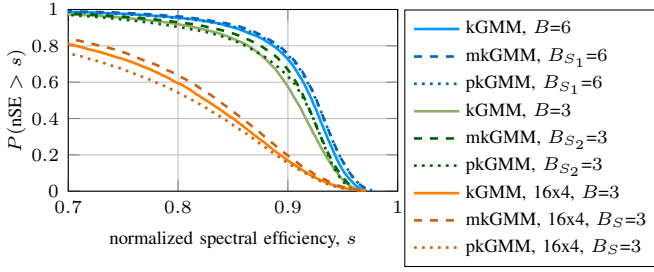
Fig. 2: Empirical complementary cumulative distribution functions (cCDFs) of the normalized spectral efficiencies for two setups using either mixture reduction techniques or the direct fitting approach **assuming perfect CSI**. Setup A: $N_{\text{tx}} = 32$ ($N_{\text{tx,h}} = 8$, $N_{\text{tx,v}} = 4$), $N_{\text{rx}} = 16$, and SNR $= 10\,\text{dB}$. Setup B: $N_{\text{tx}} = 16$ ($N_{\text{tx,h}} = 4$, $N_{\text{tx,v}} = 4$), $N_{\text{rx}} = 4$, and SNR $= 0\,\text{dB}$.

variable feedback bit lengths and eliminates the necessity of offloading a particularly trained GMM for different feedback bit lengths and thereby improves the versatility of the feedback scheme. Additionally, in Section V we discussed how model-based insights can help to effectively reduce the offloading overhead. Fig. 1 provides a flowchart of the enhanced GMM-based feedback scheme.

VII. SIMULATION RESULTS

We generate datasets for the UL and DL domain of the scenario outlined in Section II-D: $\mathcal{H}^{\text{UL}}$ and $\mathcal{H}^{\text{DL}}$. The GMM is fitted centrally at the BS using the training set $\mathcal{H} = \mathcal{H}^{\text{UL}}$ which consists of $L = 20 \cdot 10^3$ samples, cf., [5], [7], [13]–[15]. The following transmit strategies are always evaluated in the DL domain using $\mathcal{H}^{\text{DL}}$, comprised of 10^4 channels. The data samples are normalized to satisfy $\mathrm{E}[\|\boldsymbol{h}\|^2] = N = N_{\text{tx}}N_{\text{rx}}$. Additionally, we fix $\rho = 1$, enabling the definition of the SNR as $\frac{1}{\sigma_n^2}$ for all MTs, specifically when $\sigma_j^2 = \sigma_n^2, \forall j \in \mathcal{J}$.

In the single-user case, we will compare to codebook based approaches utilizing Lloyd's clustering algorithm, cf. [3], [7]. In case of MU-MIMO systems, we will either use directional information extracted from the Lloyd codebooks or we will use the random codebook approach, cf. [2], [7]. With these approaches, prior to codebook entry selection, the channel needs to be estimated. To this end, we consider three different channel estimators, which are briefly explained in the following. The recently proposed GMM-based channel estimator $\hat{\boldsymbol{h}}_{\text{GMM}}$, from [9] is one of them and utilizes the same GMM as found in Section III and calculates a convex combination of per-component linear minimum mean square error (LMMSE) estimates, cf. [7], [9]. This estimator is proven to asymptotically converge to the optimal conditional mean estimator as the number of components K is increased, cf. [9]. Another baseline is the LMMSE estimator $\hat{\boldsymbol{h}}_{\text{LMMSE}}$, where the sample covariance matrix is constructed given the set $\mathcal{H}$, cf. [7], [9], [15]. Lastly, we consider a compressive sensing estimation approach $\hat{\boldsymbol{h}}_{\text{OMP}}$ utilizing the orthogonal matching pursuit (OMP), cf. [7], [23].

A. Point-to-point MIMO

As performance measure, we utilize the normalized spectral efficiency (nSE), where the spectral efficiency achieved with
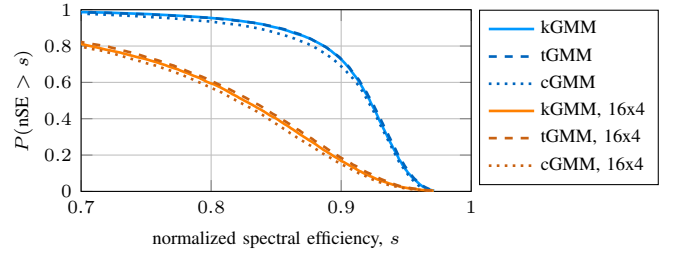
Fig. 3: Empirical cCDFs of the normalized spectral efficiencies for two setups using differently structured GMMs **assuming perfect CSI**. Setup A: $N_{\text{tx}} = 32$ ($N_{\text{tx,h}} = 8$, $N_{\text{tx,v}} = 4$), $N_{\text{rx}} = 16$, and SNR $= 10\,\text{dB}$, with $B = 6$. Setup B: $N_{\text{tx}} = 16$ ($N_{\text{tx,h}} = 4$, $N_{\text{tx,v}} = 4$), $N_{\text{rx}} = 4$, and SNR $= 0\,\text{dB}$, with $B = 3$.

a certain transmit strategy is normalized by the optimal water-filling solution, cf. [1]. The empirical cCDF $P(\text{nSE} > s)$ for the normalized spectral efficiency represents the empirical probability that the nSE surpasses a given value s.

In Fig. 2, we denote by "Setup A" a system with $N_{\text{tx}} = 32$ ($N_{\text{tx,h}} = 8, N_{\text{tx,v}} = 4$), $N_{\text{rx}} = 16$, and SNR $= 10\,\text{dB}$, and with "Setup B" a system with $N_{\text{tx}} = 16$ ($N_{\text{tx,h}} = 4, N_{\text{tx,v}} = 4$), $N_{\text{rx}} = 4$, and SNR $= 0\,\text{dB}$. In the following, we consider the Kronecker GMM ("kGMM") with full transmit- and receive-side GMMs and assume perfect CSI, i.e., the feedback information is determined via (12). For "Setup A" we fit a GMM with $K = 256$ ($B = 8$, $K_{\text{tx}} = 32$, and $K_{\text{rx}} = 8$) components and first reduce to a GMM with $K_{S_1} = 64$ ($B_{S_1} = 6$) components and continue the reduction to another one with $K_{S_2} = 8$ ($B_{S_2} = 3$) components, by either applying the merging strategy ("mkGMM") or the pruning strategy ("pkGMM"). Moreover, with "kGMM" we denote the case of directly fitting a GMM with 64 ($B = 6$, $K_{\text{tx}} = 16$, and $K_{\text{rx}} = 4$), or with 8 ($B = 3$, $K_{\text{tx}} = 4$, and $K_{\text{rx}} = 2$) components. We can observe, that both mixture reduction approaches not only enable the feedback scheme with variable bit lengths, but at the same time provide at least a similar performance as the respective direct fitting approaches. In case of "Setup B", we fit a GMM with $K = 256$ components and reduce to one with $K_S = 8$ ($B_S = 3$) components and compare to a GMM directly fitted with 8 ($K_{\text{tx}} = 4$, and $K_{\text{rx}} = 2$) components. In this setup, the merging strategy performs best, whereas the low-complexity pruning strategy yields a slightly worse performance as compared to the direct fitting approach. Altogether, the applied mixture reduction techniques enable variable bit lengths and in some cases even improve the performance as a consequence of the enhanced clustering ability, cf. [16].

In Fig. 3, consider the same two setups and denote by "tGMM" or "cGMM" Kronecker GMMs constructed by (block) Toeplitz or (block) circulant transmit- and receive-side GMMs, respectively, with 64 components ($B = 6$, $K_{\text{tx}} = 16$, and $K_{\text{rx}} = 4$) in case of "Setup A", and 8 components ($B = 3$, $K_{\text{tx}} = 4$, and $K_{\text{rx}} = 2$) in case of "Setup B". We can observe, that although the Toeplitz approximation ("tGMM") drastically reduces the offloading overhead, it achieves the same performance as the Kronecker GMM with full transmit- and receive-side GMMs ("kGMM"). The circulant approxima-
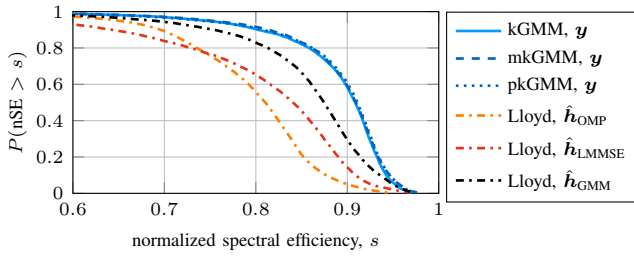
Fig. 4: Empirical cCDFs of the normalized spectral efficiencies using either mixture reduction techniques ($B = 8$ to $B_S = 6$) or the direct fitting approach ($B = 6$) for a system with $N_{\text{tx}} = 32$, $N_{\text{rx}} = 16$, SNR = 15 dB, and $n_p = 4$ pilots.
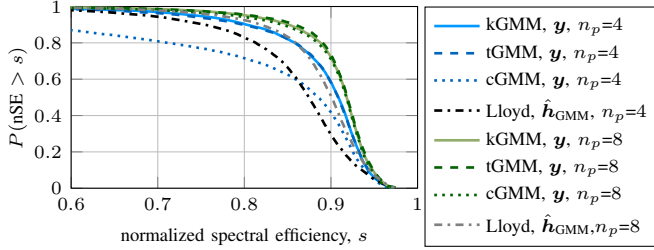
Fig. 5: Empirical cCDFs of the normalized spectral efficiencies using differently structured GMMs for a system with $N_{\text{tx}} = 32$, $N_{\text{rx}} = 16$, SNR = 15 dB, different number of pilots n_p, and $B = 6$ bits.

tion ("cGMM") with even less offloading overhead, slightly degrades the performance.

Nevertheless, assuming perfect CSI at the MT during the online phase is impractical. In the subsequent discussions, we consider imperfect CSI, i.e., systems characterized by low pilot overhead ($n_p \leq N_{\text{tx}}$). With "Lloyd, $\{\hat{\boldsymbol{h}}_{\text{GMM}}, \hat{\boldsymbol{h}}_{\text{OMP}}, \hat{\boldsymbol{h}}_{\text{LMMSE}}\}$" we depict the conventional approaches which first estimate the channel and then determine the feedback information, cf. [7]. In the remainder, the conventional approaches always utilize the same number of feedback bits of interest, i.e., B_S bits if merging or pruning is considered, or B bits if not.

In Fig. 4, we simulate a setup with $N_{\text{tx}} = 32$ ($N_{\text{tx,h}} = 8, N_{\text{tx,v}} = 4$), $N_{\text{rx}} = 16$, SNR = 15 dB, and $n_p = 4$ pilots. We again consider a GMM with $K = 256$ ($B = 8$, $K_{\text{tx}} = 32$, and $K_{\text{rx}} = 8$) components and reduce to a GMM with $K_S = 64$ ($B_S = 6$) components, by applying the merging strategy ("mkGMM") or the pruning strategy ("pkGMM"). We can observe, that the GMM-based feedback approach ("kGMM, $\boldsymbol{y}$"), which circumvents explicit channel estimation, is superior as compared to the baselines and provides a higher robustness against CSI imperfections. The proposed merging and pruning strategies exhibit a similar robustness.

In Fig. 5, we have $N_{\text{tx}} = 32$ ($N_{\text{tx,h}} = 8, N_{\text{tx,v}} = 4$), $N_{\text{rx}} = 16$, SNR = 15 dB, and $n_p \in \{4, 8\}$ pilots and depict differently structured GMMs with $K = 64$ ($K_{\text{tx}} = 16$, and $K_{\text{rx}} = 4$) components. The Toeplitz approximation ("tGMM") with a reduced number of parameters achieves the same performance as compared to the Kronecker GMM with full transmit- and receive-side GMMs ("kGMM"), irrespective of the number of pilots. With $n_p = 4$, the proposed approach "tGMM" attains the same performance as the conventional Lloyd approach with twice as much pilots ($n_p = 8$). This shows, the great potential of the enhanced GMM-based feed-
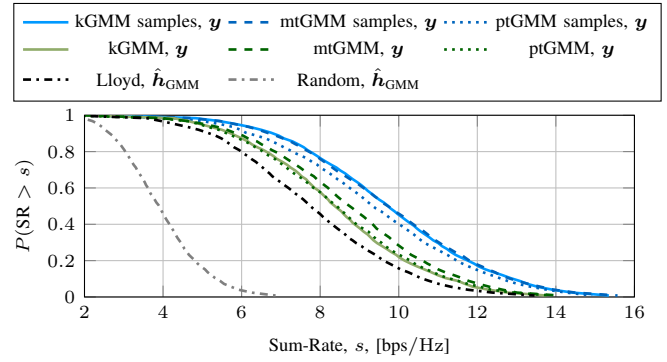
Fig. 6: Empirical cCDFs of the sum-rate using either mixture reduction techniques ($B = 8$ to $B_S = 6$) combined with Toeplitz structured GMMs or the direct fitting approach ($B = 8$) when the iterative WMMSE or the SWMMSE are utilized, for a system with $N_{\text{tx}} = 16$, $N_{\text{rx}} = 4$, $J = 4$ MTs, SNR = 5 dB, and $n_p = 8$ pilots.

back scheme in systems with reduced pilot overhead. Interestingly, in case of the circulant approximation ("cGMM") a performance degradation can be observed if $n_p = 4$. It seems that the expressivity of the circulant GMM with a very low number of parameters is too restrictive to be applied for systems with a few pilots only. Since the Toeplitz approach provides a higher robustness, we will restrict our further analysis to it in the remainder.

B. Multi-user MIMO

For the multi-user scenario, we utilize the sum-rate as performance metric, cf. [7]. The presented results are based on 2,500 constellations, where for each constellation, we randomly select J MTs from our evaluation set $\mathcal{H}^{\text{DL}}$. We employ the empirical cCDF $P(\text{SR} > s)$ of the sum-rate to illustrate the empirical probability of the sum-rate (SR) exceeding a given value s. Although the GMM-based feedback scheme can be used in combination with non-iterative precoding algorithms, in the following we restrict our analysis to the iterative WMMSE and to the SWMMSE in order to design the precoders, since the performance with these methods is generally better, cf. [7].

In the subsequent discussion, we refer with "GMM, $\boldsymbol{y}$" to the case where the observations $\boldsymbol{y}_j$ are used at each MT j to determine a feedback index utilizing the GMM feedback encoding approach, cf. (13). The channel of each MT is then represented by the subspace information extracted from the GMM codebook, cf. Section III-C. For the sake of clarity in the legend, we omit the index j. With "$\{$Lloyd, Random$\}$, $\{\hat{\boldsymbol{h}}_{\text{GMM}}, \hat{\boldsymbol{h}}_{\text{OMP}}, \hat{\boldsymbol{h}}_{\text{LMMSE}}\}$", we denote the cases where the channel is estimated at each MT and subsequently the feedback information is determined using either the directional Lloyd codebook or the random codebook approach, cf. [7]. These methods use the iterative WMMSE, cf. [20, Algorithm 1]. Furthermore, with "GMM samples, $\boldsymbol{y}$" we refer to the case, where we generate samples representing the distribution of each MT using the GMM and feed these samples to the SWMMSE algorithm, cf. Section III-C. The maximum number of iterations is $I_{\max} = 300$ for both approaches.

In the remainder, we combine both, the Toeplitz approximation and the mixture reduction techniques in a setup with
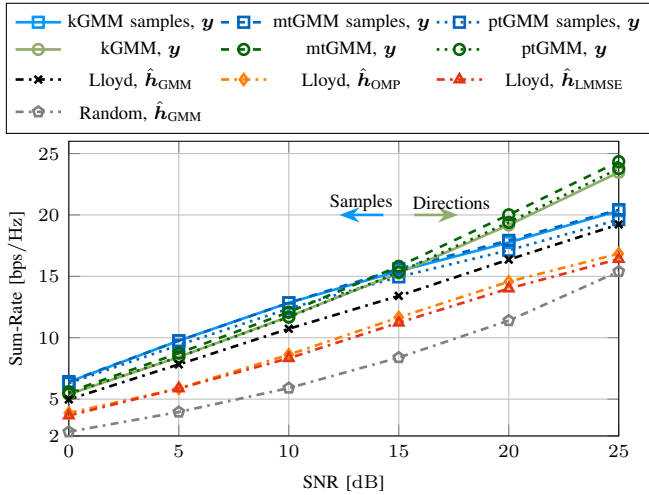
Fig. 7: The average sum-rate over the SNR using either mixture reduction techniques ($B = 8$ to $B_S = 6$) combined with Toeplitz structured GMMs or the direct fitting approach ($B = 6$) when the iterative WMMSE or the SWMMSE are employed, for a system with $N_{\mathrm{tx}} = 16$, $N_{\mathrm{rx}} = 4$, $J = 4$ MTs, and $n_p = 8$ pilots.

$N_{\mathrm{tx}} = 16$ ($N_{\mathrm{tx,h}} = 4, N_{\mathrm{tx,v}} = 4$) and $N_{\mathrm{rx}} = 4$, and $J = 4$ users. In particular, we fit a Kronecker GMM constructed by (block) Toeplitz transmit- and receive-side GMMs, with $K = 256$ components and reduce to a GMM with $K_S = 64$ ($B_S = 6$) components denoted by "mtGMM" and "ptGMM", and compare to a GMM directly fitted with 64 ($K_{\mathrm{tx}} = 16$, and $K_{\mathrm{rx}} = 4$) components with full transmit- and receive-side GMMs ("kGMM"). In Fig. 6, with $\mathrm{SNR} = 5\,\mathrm{dB}$ and $n_p = 8$ pilots, we can see that the pruning and merging strategy in combination with the Toeplitz structured covariances in case of the directional (subspace) approach, i.e., "ptGMM, $\boldsymbol{y}$" and "mt-GMM, $\boldsymbol{y}$", perform similarly or even better than the "kGMM, $\boldsymbol{y}$" and outperform the conventional methods "{Lloyd, Random}, $\hat{\boldsymbol{h}}_{\mathrm{GMM}}$", by far. With the generative modeling approach, the merging method "mtGMM samples, $\boldsymbol{y}$" performs equally well as "kGMM samples, $\boldsymbol{y}$", whereas the pruning method "ptGMM samples, $\boldsymbol{y}$" performs slightly worse.

A similar behaviour is present in Fig. 7, where we still consider the same setting with $n_p = 8$ pilots, but vary the SNR and depict the sum-rate averaged over all constellations. Interestingly, with an increasing SNR, the gap between "mtGMM, $\boldsymbol{y}$" and "kGMM, $\boldsymbol{y}$" increases. Similarly, the gap between "ptGMM samples, $\boldsymbol{y}$" and "kGMM samples, $\boldsymbol{y}$" increases with larger SNR values. As reported in [7], adopting the generative modeling approach for joint precoder design is advantageous in scenarios characterized by low to moderate SNR levels, and for larger SNR values the directional approach is beneficial. This property can be similarly observed if the merging or pruning procedures are applied, and is illustrated by the arrows in Fig. 7. Altogether, the enhanced GMM-based feedback scheme exhibits superior performance compared to the baselines in a multi-user system with reduced pilot overhead.

VIII. CONCLUSION

In this work, we enhanced the versatile GMM-based feedback from [7] scheme by enabling variable bit lengths and incorporating further model-based structural constraints to reduce the offloading overhead. To this end, we analyzed two mixture reduction techniques, i.e., one pruning and one merging strategy and found out, that both approaches enable the scheme with variable bit lengths and allow for a trade-off between complexity and performance. Moreover, numerical results showed the remarkable performance of the combination of mixture reduction techniques with structured GMMs.

REFERENCES

[1] D. J. Love, R. W. Heath, V. K. N. Lau, D. Gesbert, B. D. Rao, and M. Andrews, "An overview of limited feedback in wireless communication systems," *IEEE J. Sel. Areas Commun.*, vol. 26, no. 8, pp. 1341–1365, 2008.

[2] N. Ravindran and N. Jindal, "Limited feedback-based block diagonalization for the MIMO broadcast channel," *IEEE J. Sel. Areas Commun.*, vol. 26, no. 8, pp. 1473–1482, 2008.

[3] V. Lau, Y. Liu, and T.-A. Chen, "On the design of MIMO block-fading channels with feedback-link capacity constraint," *IEEE Trans. Commun.*, vol. 52, no. 1, pp. 62–70, 2004.

[4] J. Jang, H. Lee, I.-M. Kim, and I. Lee, "Deep learning for multi-user MIMO systems: Joint design of pilot, limited feedback, and precoding," *IEEE Trans. Commun.*, vol. 70, no. 11, pp. 7279–7293, 2022.

[5] N. Turan, M. Koller, S. Bazzi, W. Xu, and W. Utschick, "Unsupervised learning of adaptive codebooks for deep feedback encoding in FDD systems," in *55th Asilomar Conf. Signals, Syst., Comput.*, 2021, pp. 1464–1469.

[6] N. Turan, M. Koller, B. Fesl, S. Bazzi, W. Xu, and W. Utschick, "GMM-based codebook construction and feedback encoding in FDD systems," in *56th Asilomar Conf. Signals, Syst., Comput.*, 2022, pp. 37–42.

[7] N. Turan, B. Fesl, M. Koller, M. Joham, and W. Utschick, "A versatile low-complexity feedback scheme for FDD systems via generative modeling," *IEEE Trans. Wireless Commun.*, 2023, to be published, arXiv preprint: 2304.14373.

[8] T. T. Nguyen, H. D. Nguyen, F. Chamroukhi, and G. J. McLachlan, "Approximation by finite mixtures of continuous density functions that vanish at infinity," *Cogent Math. Statist.*, vol. 7, no. 1, p. 1750861, 2020.

[9] M. Koller, B. Fesl, N. Turan, and W. Utschick, "An asymptotically MSE-optimal estimator based on Gaussian mixture models," *IEEE Trans. Signal Process.*, vol. 70, pp. 4109–4123, 2022.

[10] B. Fesl, N. Turan, M. Joham, and W. Utschick, "Learning a Gaussian mixture model from imperfect training data for robust channel estimation," *IEEE Wireless Commun. Lett.*, 2023.

[11] B. Fesl, M. Joham, S. Hu, M. Koller, N. Turan, and W. Utschick, "Channel estimation based on Gaussian mixture models with structured covariances," in *56th Asilomar Conf. Signals, Syst., Comput.*, 2022, pp. 533–537.

[12] N. Turan, B. Fesl, M. Grundei, M. Koller, and W. Utschick, "Evaluation of a Gaussian mixture model-based channel estimator using measurement data," in *Int. Symp. Wireless Commun. Syst. (ISWCS)*, 2022.

[13] W. Utschick, V. Rizzello, M. Joham, Z. Ma, and L. Piazzi, "Learning the CSI recovery in FDD systems," *IEEE Trans. Wireless Commun.*, vol. 21, no. 8, pp. 6495–6507, 2022.

[14] N. Turan, M. Koller, V. Rizzello, B. Fesl, S. Bazzi, W. Xu, and W. Utschick, "On distributional invariances between downlink and uplink MIMO channels," in *25th Int. ITG Workshop Smart Antennas (WSA)*, 2021.

[15] B. Fesl, N. Turan, M. Koller, M. Joham, and W. Utschick, "Centralized learning of the distributed downlink channel estimators in FDD systems using uplink data," in *25th Int. ITG Workshop Smart Antennas (WSA)*, 2021.

[16] C. Hennig, "Methods for merging Gaussian mixture components," *Adv. Data Anal. Classif.*, vol. 4, p. 3–34, 2010.

[17] A. Runnalls, "Kullback-Leibler approach to Gaussian mixture reduction," *IEEE Trans. Aerosp. Electron. Syst.*, vol. 43, no. 3, pp. 989–999, 2007.

[18] S. Jaeckel, L. Raschkowski, K. Börner, and L. Thiele, "Quadriga: A 3-d multi-cell channel model with time evolution for enabling virtual field trials," *IEEE Trans. Antennas Propag.*, vol. 62, no. 6, pp. 3242–3256, 2014.

[19] C. M. Bishop, *Pattern Recognition and Machine Learning (Information Science and Statistics)*. Berlin, Heidelberg: Springer-Verlag, 2006.

[20] Q. Hu, Y. Cai, Q. Shi, K. Xu, G. Yu, and Z. Ding, "Iterative algorithm induced deep-unfolding neural networks: Precoding design for multiuser MIMO systems," *IEEE Trans. Wireless Commun.*, vol. 20, no. 2, pp. 1394–1410, 2021.

[21] M. Razaviyayn, M. S. Boroujeni, and Z.-Q. Luo, "A stochastic weighted MMSE approach to sum rate maximization for a MIMO interference channel," in *IEEE 14th Int. Workshop Signal Process. Adv. Wireless Commun. (SPAWC)*, 2013, pp. 325–329.

[22] D. F. Crouse, P. Willett, K. Pattipati, and L. Svensson, "A look at Gaussian mixture reduction algorithms," in *14th Int. Conf. Inf. Fusion*, 2011.

[23] A. Alkhateeb, G. Leus, and R. W. Heath, "Compressed sensing based multi-user millimeter wave systems: How many measurements are needed?" in *IEEE Int. Conf. Acoust., Speech Signal Process. (ICASSP)*, 2015, pp. 2909–2913.